Integration of quantum dot light sources

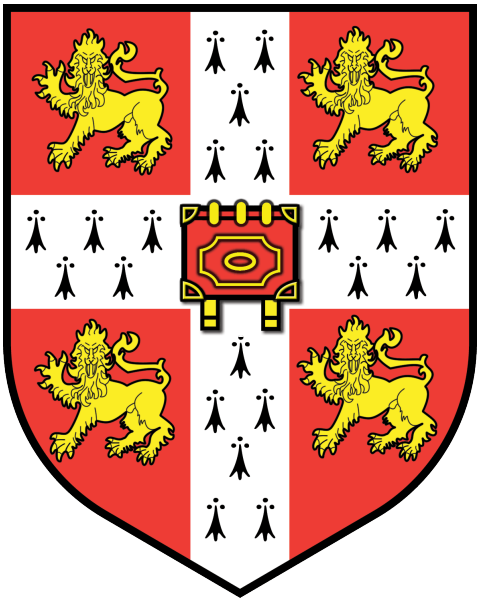

Eoin Murray

Magdalene College

Department of Physics

University of Cambridge

2015

A first year report submitted for the degree of

Doctor of Philosophy (Probationary)

Acknowledgements

This project was very much a team effort and I would first like to thank all the members of the integration project team. Thanks to David Ellis for designing and fabricating the devices, the devices were fabricated at the Cavendish and the e-beam lithography was undertaken by Jonathan Griffiths. Thanks to Thomas Meany for packaging the hybrid device and taking measurements, Frederick Floether for designing the devices, Jamie Lee for assisting with measurements and to Anthony Bennet for designing and taking measurements. Thanks also for Ian Farrer and the staff at the Cavendish for growing wafers. Thanks to Andrew Shields and David Ritchie for giving me this opportunity to study for this PhD. This project was supported by the Initial Training Network PICQUE under the European Commission Marie Curie Actions.

Abstract

Fundamental to the future of quantum photonics is the ability to create integrated devices. An integrated chip offers intrinsic stability and compactness. This makes it inherently more scalable than a bulk optics approach. Quantum dots (QDs) are a developing on-chip source of single photons. This project aims to take quantum dots embedded in a III-V material and combine them with integrated waveguide components. The InAs QDs are grown in GaAs substrate and are bonded to a SiON based waveguide platform. This approach has potential for realization of an efficient coupling between the quantum dots and the waveguides and then on-chip manipulation of the emitted photons. In this report, the results thus far will be presented and proposals for future designs will be discussed.

Publications resulting from this work

Quantum photonics hybrid integration platform

E. Murray, D. J. P. Ellis, T. Meany, F. F. Floether, J. P. Lee, J. P. Griffiths, G. A. C. Jones, I. Farrer, D. A. Ritchie, A. J. Bennett, and A. J. Shields.

Applied Physics Letters 107.17 (2015): 171108.

Cavity-enhanced coherent light scattering from a quantum dot A. J. Bennett, J. P. Lee, D. J. P. Ellis, T. Meany, **E. Murray**, F. F. Floether, J. P. Griffiths, I. Farrer, D. A. Ritchie, and A. J. Shields.

arXiv pre-print: 1508.01637v1

Conferences

Quantum dots for quantum information science,

E. Murray

PICQUE Integrated Quantum Photonics Workshop, 7-9 January 2015, Oxford, UK

Quantum photonics hybrid integration platform

E. Murray, D. J. P. Ellis, T. Meany, F. F. Floether, J. P. Lee, J. P. Griffiths, G. A. C. Jones, I. Farrer, D. A. Ritchie, A. J. Bennett, and A. J. Shields.

Best talk awarded PICQUE Roma Scientific School, 6-10 July 2015, Rome, Italy

Contents

Chapter 1

Introduction and theory.

Linear optical quantum computing (LOQC) has been proven to be computationally efficient with a single photon source and a series of beamsplitters and phase shifters [1]. Some implementations of two photon gates have been realised with bulk optics [2], however a scalable LOQC is unfeasible with bulk optics and an integrated technology is needed [3]. Semiconductor waveguides with integrated quantum dots (QD) are a promising solution. Semiconductor III-V QDs have been shown to have good, bright, single photon emission [4], can emit indistinguishable and entangled photons [5, 6], can be site-controlled [7] and are compatible with semiconductor foundry techniques. Progress is being made to embed the QDs into integrated waveguide platforms. Integrated photonics offers the potential for true scalability due to component miniaturisation. Stability is intrinsic to the platform and offers a reduction in complexity and size of the device [8]. Many of the elements needed for LOQC can be manufactured on-chip, high fidelity beam splitters and Mach Zehnder interferometers (MZIs) can be made in various semiconductors [9, 10, 11] as well as on-chip detectors [12, 13] however further work is needed to integrate these components on with a quantum light source.

1.1 Introduction to Quantum dots

Semiconductor quantum dots (QDs) are islands of material of a certain material surrounded by a material of a higher band gap. The QD region is a three dimensional structure which confines

carriers in zero dimensions. This confinement gives rise to discrete energy levels inside the QD.

Normally a QD will confine two electron levels and two hole levels, more may be accomodated in a larger QD. Each level will only confine two carriers due to the Pauli exclusion principle. Figure 1.1 shows the electronic structure of a QD. An electron excited to the conduction band leave a hole in the valence band and ins referred to as an e-h pair. An e-h pair confined in the QD is referred to as an exciton, two e-h pairs is a biexciton. When there is an imbalance in the number of electrons and holes a charged exciton is created. Electron-hole pairs can be excited into the quantum dot by numberous methods - primarily electro and photo-excitation. In the non-resonant case, carriers are created in the visinity of the QD by an above band excitation laser or an electric current. These carriers will relax into the available quantum potentials, the lowest energy of which is typically the QD.

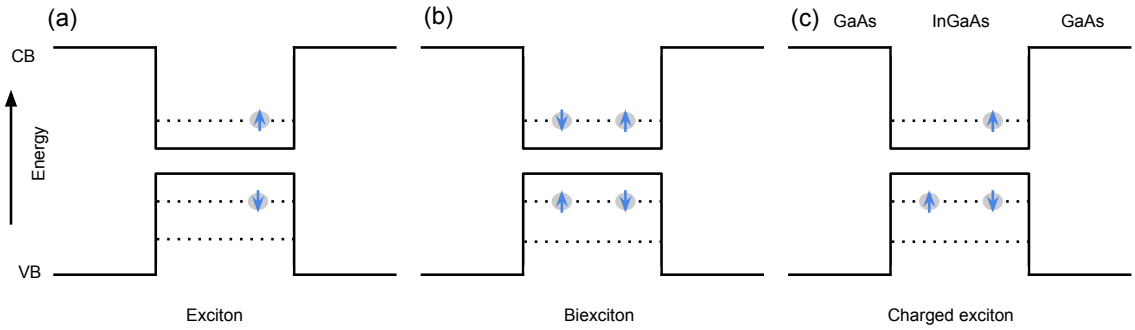

Figure 1.1: Electronic structure of a quantum dot. (a) An exciton e-h pair. (b) A biexciton with two e-h pairs. (c) An exciton with an extra hole making a positively charged exciton.

The discrete energy levels in the QD give rise to clean, sharp emission lines. There is a well defined energy for each transition and as such the emitted photons have a well defined wavelength, limited by the lifetime of the state.

1.1.1 Single photon emission from Quantum dots

The angular momentum of an electron is $\pm 1/2$ and for a hole is $\pm 3/2$. The e-h pair can combine to make a state with spin ± 1 for photon emission and ± 2 for nonradiative recombination. The energy

of the emitted photon corresponds to the energy of its original excitonic state. Thus the emitted photons can be spectrally filtered to analyse the emission from only one excitonic state.

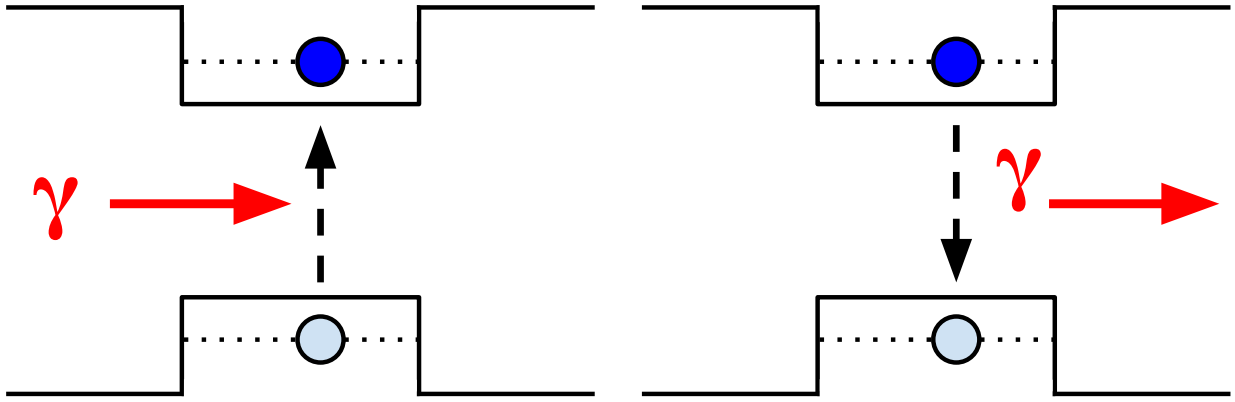

Figure 1.2: Single photon emission process in a quantum dot.

For a light source with Poissonian emission statistics such as a laser true single photon emission can not be achieved even with significant attenuation because the probaility for multi photon emission still exists. In the case of a quantum dot since each excitonic energy level can only accept a fixed number of carriers and after photon emission there is a finite time which must pass before more carriers can be captured true single photon emission is possible. This process is shown schematically in Figure 1.2. This single photon emission can be verified by measuring the two photon second order correlation function

$$g^{(2)}(\tau) = \frac{\langle I(t)I(t+\tau)\rangle}{\langle I(t)\rangle \langle I(t+\tau)\rangle} \tag{1.1}$$

This is done by doing a Hanbury Brown Twiss measurement. A stream of single photons impinge on a 50:50 beamsplitter. The two outputs of the beamsplitters are sent to single photon detectors. One of the detector signals is delayed by a time τ in order to measure both positive and negative correlation times. If the source is a true single photon source there will be a lack of coincidence clicks on both detectors when $\tau = 0$, and thus $g^{(2)}(0)$ will be zero. Single photon emission from QDs has been demonstrated under a wide range of excitation conditions - DC and AC electrical excitation, continous wave (cw) and pulsed lasers at above band, quasi-resonant and resonant energies.

1.2 Semiconductor waveguides

A dielectric waveguide is a core material surrounded by a material of lower refractive index. The surrounding material is known as the waveguide cladding. Here the theory is set out as in Integrated Photonics by Saleh and Teich [14]. As an introduction to the design of waveguides in this section the propogation of light in a symmetric dielectric slab waveguide will be discussed. A core slab of refractive index n_1 is clad by two slabs of refractive index n_2. This structure is shown in Figure 1.3. The critical angle for the total internal reflection of light is derived from Snells law to be

$$\theta_c = \arcsin \frac{n_1}{n_2}. \tag{1.2}$$

When light impinges on the boundary of n_1 and n_2 with an angle less than θ_c then it is reflected. Figure 1.3 shows a guided and unguided ray of light. The unguided ray hits the boundary with an angle greater than θ_c and therefore some of the light refracts, therefore losing some of the light at each reflection causing the ray to eventually vanish. The guided ray hits the boundary at an angle less than θ_c and reflects without any loss of power and will propagate along the core.

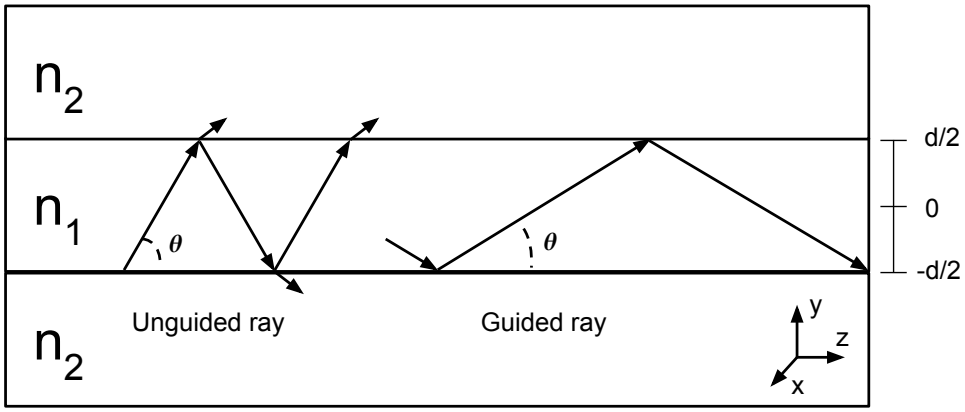

Figure 1.3: Light ray propagation in a planar dielectric waveguide.

To understand the waveguide modes in the structure assume there is a transverse electromagnetic (TEM) plane wave propogating in the waveguide core. This TEM wave has a wavelength $\lambda = \lambda_0/n_1$ where λ_0 is the free space wavelength. The wave is reflecting each time at the boundary with an

angle less than θ_c so the wave propagates in the core without loss of power. With each reflection the wave lags behind the original by a distance $2d\sin\theta$ [14]. There is also a phase ϕ_r change induced by each internal reflection. There is now a self-consistancy condition imposed upon the reflected wave. As the wave reflects twice it reproduces itself, waves which satisfy this condidion are known as eigenmodes, or modes of the waveguide. The wave interferes with itself a pattern is created which does not change with $\hat{z}$. Due to this self-consistency the phase shift between the waves is zero or a multiple of 2π, giving rise to the condition

$$2k_y d - 2\phi_r = 2\pi m, \qquad m = 0, 1, 2, ... \tag{1.3}$$

where $k_y = n_1 k_0 \sin\theta$. The phase shift ϕ_r in the transverse electric (TE) case due to total internal reflection is given by

$$\tan\frac{\phi_r}{2} = \sqrt{\frac{\sin^2\theta_c}{\sin^2\theta} - 1}. \tag{1.4}$$

Combining this with Equation 1.3 it is deduced that

$$\tan\left(\pi\frac{d}{\lambda}\sin\theta - m\frac{\pi}{2}\right) = \sqrt{\frac{\sin^2\theta_c}{\sin^2\theta} - 1} \tag{1.5}$$

This equation is trancendental and can be solved graphically, this solution is shown in Figure 1.4. The LHS is a set of tan, when m is even, and cot functions, when m is odd. Each LHS segment corresponds to a mode in the waveguide. When the LHS crosses the x-axis, indicated by the semicircles, $\sin\theta_m$ can be determined. The distance between these intersections is $\lambda/2d$. The solution for transverse magnetic (TM) is very similar, with just a different phase change upon reflection ϕ_r. This information can be used to deduce how many TE modes are in a waveguide of a given size d. The number of modes M is given by the amount of segments of width $\lambda/2d$ exist before $\sin\theta$ reaches the value $\sin\theta_c$.

$$M = \frac{\sin\theta_c}{\lambda/2d}, \tag{1.6}$$

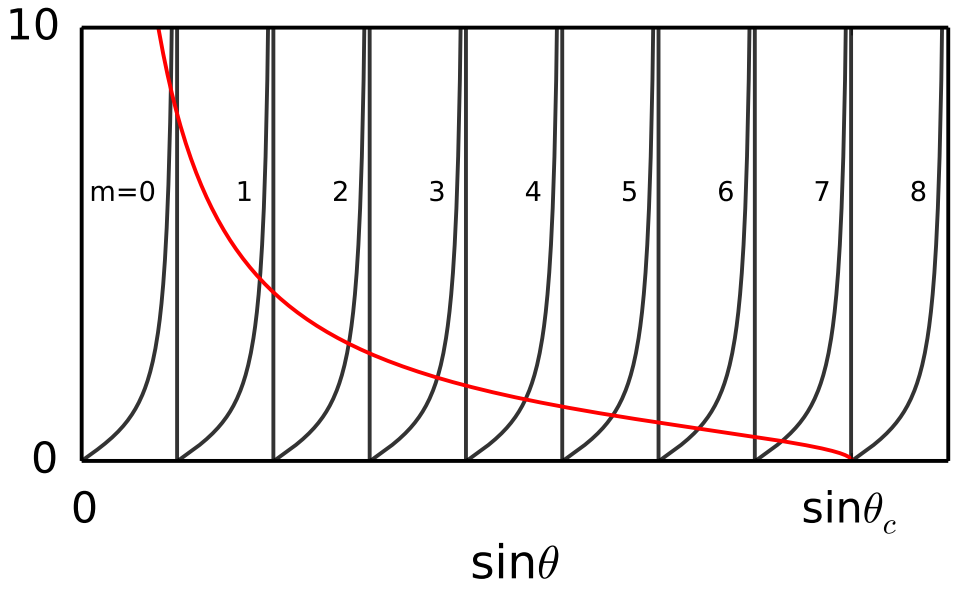

Figure 1.4: Graphical solution of Equation 1.5. The black line is the LHS of the equation and the red line is the RHS. Each LHS segment corresponds to a mode in the waveguide.

rounded up to the nearest integer. By substituting $\cos\theta_c = n_2/n_1$ into Equation 1.2 it is seen that

$$M = 2\frac{d}{\lambda}\mathrm{NA} \tag{1.7}$$

where

$$\mathrm{NA} = \sqrt{n_1^2 - n_2^2} \tag{1.8}$$

is the numerical aperture of the waveguide. The NA defines the range of angle from which the waveguide can collect light. Equation is extremely important in waveguide design because it defines the single-mode cutoff for when $M \leq 1$. This impacts the choice of d and the wavelength for which the waveguide is single mode or multimode. Single mode waveguides are generally more useful for quantum optics because they allow two photon interference between light coming in from two single mode channels, this allows the operation of directional couplers and Mach Zehnder interferometers. Single mode optical fibres have lower loss in the telecommunications wavelength ranges so is better

suited to long distance communication.

1.2.1 Two dimensional waveguides

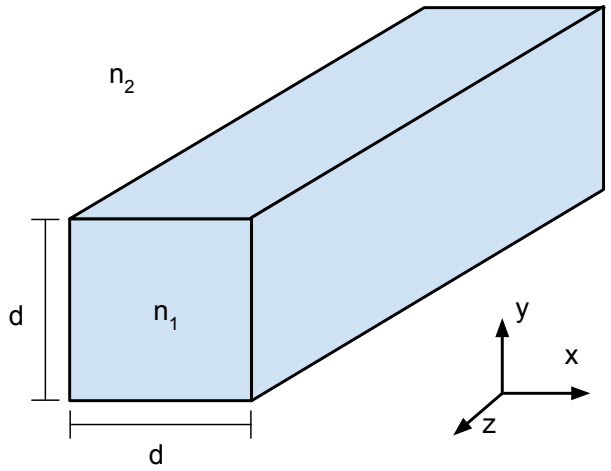

Figure 1.5: Index structure of a waveguide which confines light in two dimensions. The light is confined in $\hat{x}$ and $\hat{y}$ but is free to propagate in the $\hat{z}$ direction.

A two dimensional dielectric waveguide is one which confines light along two axes and allows the light to free propagate along the third axis. A schematic of a rectangular waveguide is shown in Figure 1.5. The modes and number of modes can be derived in a similar fashion as for the planar dielectric waveguide and shall just be quoted here [14]. The number of modes in a two dimensional waveguide can be approximated by

$$M \approx \frac{\pi}{4}\left(\frac{2d}{\lambda_o}\right)^2 \mathrm{NA}^2. \tag{1.9}$$

This approximation holds well for multimode waveguides, but loses accuracy near the single mode boundary. Design of single mode two dimensional waveguides generally needs to be solved computationally.

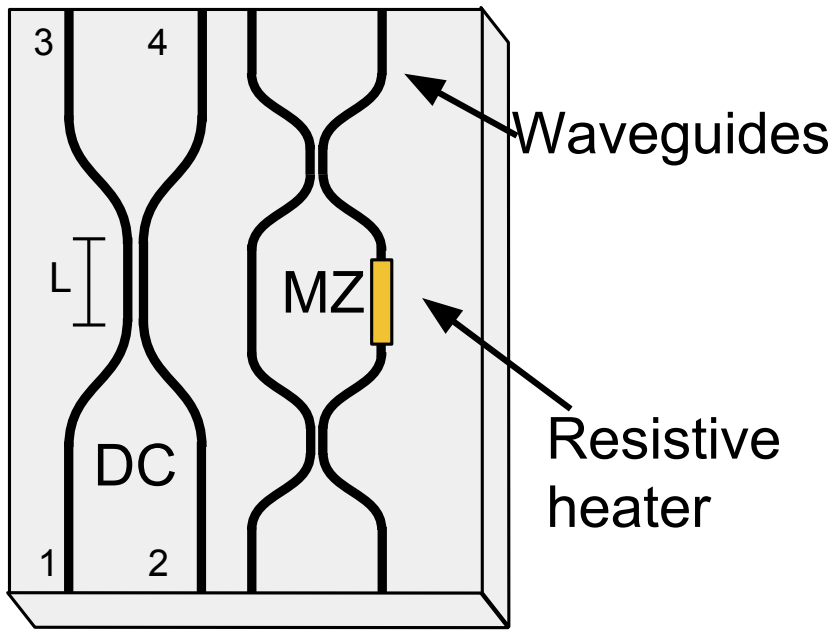

Figure 1.6: Two common waveguide devices, a directional coupler and a Mach Zehnder interferometer. The numbers on the directional couplers indicate input and output ports which shall be reference in the text, equivalent ports shall be used for the Mach Zehnder interferometer.

1.2.2 Directional couplers and Mach Zehnder interferometers

Figure 1.6 shows the schematic of two waveguide devices used frequently throughout this project. A directional coupler (DC) is a photonic device which splits the power between two output ports with a well defined coupling ratio between the ports. Two waveguides are brought close enough so that the evanescent fields overlap. The waveguides are assumed to be single mode. It can be derived that the power in each port 3 and 4 in Figure 1.6 as a result of light of power P_1 being injected to the coupler from port 1 is

$$P_3(z) = P_1 \cos^2 cz \tag{1.10}$$

$$P_4(z) = P_1 \sin^2 cz \tag{1.11}$$

Where z is the propagation direction and c is the coupling coefficient related to the index contrast of the waveguide, the separation d between the waveguides in the interaction region and the operating

wavelength.

A Mach Zehnder interferometer (MZI) is a sequence of two DCs in parallel. The light splits 50/50 into two arms by the first DC. On one of the arms is a local refractive index changing element, this can be a electrode to take advantage of the electro-optic effect or heater, for the thermo-optic effect. Here it shall be assumed to be a heater. This element changes the local refractive index in the arms. This causes a phase mismatch between the light propagating in each arm so that the light will constructively or destructively interfere at the second DC. By tuning the heater this phase can be chosen an light can be arbitrarily coupled between ports 3 and 4. This is called a Mach Zehnder interferometer switch or modulator. These are used extensively in telecommunications to route signals between different channels.

1.3 Integrated quantum devices

Semiconductor quantum dots and waveguides are interesting technologies on their own. However this thesis focuses on the combination of these technologies to create a platform capable of making working integrated quantum devices in the future.

In the approach of these thesis laid out in Chapter 2 and 3, we attach a QD filled GaAs chip to the end of a SiON based photonic circuit. This approach allows us to make custom designed photonic circuits, which are fabricated seperately from the QD quantum light source. The circuits are made up of a series of MZI's. This thesis focuses on the initial fabrication and demonstration of the platform. In the next phase of reseach there are many target circuits which are interesting for quantum telecommunications which have been demonstrated with QD's with bulk optics, but not yet reproduced on an integrated device. CNOT gates[15], quantum relays' [16], quantum amplifiers [17, 18], NOON state generations [19] and various combiners and splitters.

1.3.1 NOON states and quantum sensing

This section will describe a useful application of quantum sources and quantum circuits, generating a NOON state. The dynamics of a NOON state as is passed through a MZI allow it to be super sensitive to phase changes in the MZI. A NOON state is a many particle quantum entangled state. It is represented as:

$$|\psi\rangle = |N\rangle_a |0\rangle_b + e^{iN\theta} |0\rangle_a |N\rangle_b \tag{1.12}$$

this state is a superposition of N particles in mode a and 0 particles in mode b and vica-versa. The particles need to be bosonic and in this case the quantum particles are photons.

To generate this state using photonics we consider the state generated by photons propagating through an MZI. In the single photon case, single-photon interference occurs from the path length difference in the two arms of the MZI. One of the photon modes gathers a phase shift $\Delta\phi$ and causes the detection probabilities of the MZI output arms to change.

The probabilities become $P_1 = 1 + \cos\Delta\phi$ and $P_2 = 1 + \sin\Delta\phi$.

This interference is generalised by Hong-Ou-Mandel interence [**?**] for multiple photons. The biphoton state must then be represented by a path entangled state:

$$|\psi\rangle = |2\rangle_a |0\rangle_b + e^{i2\theta} |0\rangle_a |2\rangle_b \tag{1.13}$$

In this case the oscillation of the detection probabilities depending on phase is twice as fast. $P_{1,1} = 1 + \cos 2\Delta\phi$ and $P_{2,2} = 1 + \sin 2\Delta\phi$.

This path encoded biphoton state is the same a two particle NOON state. It is seen that the phase modulation increases linearly with the number of particles in the state $N\Delta\phi$. This would allow smaller phase changes to be detected faster by some quantum sensor, this is known as superresolution.

It can also be seen that the error in the phase measurement becomes smaller for larger N. Consider the observable

$$O = |N,0\rangle \langle 0,N| + |0,N\rangle \langle N,0| \tag{1.14}$$

The error in the phase becomes

$$\Delta\phi = \frac{\Delta O}{|d\langle O\rangle / d\phi|} = \frac{1}{N} \tag{1.15}$$

Thus the phase error decreases with increasing particle number, this is known as supersensitivity.

NOON state super resolution can be achieved experimentally using quantum dots and an integrated photonic circuit [19]. QDs are resonantly excited in order to achieve long coherence times and good two photon interference visibilities.

The photons are generated sequentially from the QD, they are directed to a 50:50 beamsplitter where one are is delayed. This causes 25to be time synched in parallell.

The two photons are then sent into a MZI, whereby detecting the coincidences from the outputs the phase of the MZI can be determined accurately.

In an integrated photonic circuit MZI, the phase of one arm is changed by inducing a refractive index change on that arm. This refractive index change causes a change in the phase of the circuit. This phase change is then measured with high sensitivity by the NOON state, allowing a supersensitive measurement of whatever caused the refractive index change.

Any component which changes the refractive index of one arm can then be sensed.

For example, placing a conducting gold strip over one arm will induce a refractive index change when there is a current run through the strip. This current can then be supersensed.

If a microfluidic channel is placed in the path of the light going down one arm of the MZI, the fluid will have a different refractive index depending on its contents. This can be used to sense trace

amounts of components inside the fluid [**?**].

Bibliography

[1] Emanuel Knill, Raymond Laflamme, and Gerald J Milburn. A scheme for efficient quantum computation with linear optics. *Nature*, 409(6816):46–52, 2001.

[2] Jeremy L O'Brien, Geoffrey J Pryde, Andrew G White, Timothy C Ralph, and David Branning. Demonstration of an all-optical quantum controlled-not gate. *Nature*, 426(6964):264–267, 2003.

[3] Jacques Carolan, Chris Harrold, Chris Sparrow, Enrique Martín-López, Nicholas J Russell, Joshua W Silverstone, Peter J Shadbolt, Nobuyuki Matsuda, Manabu Oguma, Mikitaka Itoh, et al. Universal linear optics. *arXiv preprint arXiv:1505.01182*, 2015.

[4] A. J. Bennett, D. C. Unitt, P. Atkinson, D. A. Ritchie, and A. J. Shields. High performance single photon sources from photolithographically defined pillar microcavities. *Opt. Express*, 13(1):50–55, Jan 2005.

[5] Yu-Ming He, Yu He, Yu-Jia Wei, Dian Wu, Mete Atatüre, Christian Schneider, Sven Höfling, Martin Kamp, Chao-Yang Lu, and Jian-Wei Pan. On-demand semiconductor single-photon source with near-unity indistinguishability. *Nature nanotechnology*, 8(3):213–217, 2013.

[6] RM Stevenson, CL Salter, J Nilsson, AJ Bennett, MB Ward, I Farrer, DA Ritchie, and AJ Shields. Indistinguishable entangled photons generated by a light-emitting diode. *Physical review letters*, 108(4):040503, 2012.

[7] Gediminas Juska, Valeria Dimastrodonato, Lorenzo O Mereni, Agnieszka Gocalinska, and Emanuele Pelucchi. Towards quantum-dot arrays of entangled photon emitters. *Nature Photonics*, 7(7):527–531, 2013.

[8] Alberto Politi, Jonathan CF Matthews, Mark G Thompson, and Jeremy L O'Brien. Integrated quantum photonics. *Selected Topics in Quantum Electronics, IEEE Journal of*, 15(6):1673–1684, 2009.

[9] Jianwei Wang, Alberto Santamato, Pisu Jiang, Damien Bonneau, Erman Engin, Joshua W Silverstone, Matthias Lermer, Johannes Beetz, Martin Kamp, Sven Höfling, et al. Gallium arsenide (gaas) quantum photonic waveguide circuits. *Optics Communications*, 327:49–55, 2014.

[10] Yanfeng Zhang, Loyd McKnight, Erman Engin, Ian M. Watson, Martin J. Cryan, Erdan Gu, Mark G. Thompson, Stephane Calvez, Jeremy L. OBrien, and Martin D. Dawson. Gan directional couplers for integrated quantum photonics. *Applied Physics Letters*, 99(16):–, 2011.

[11] Alberto Politi, Martin J Cryan, John G Rarity, Siyuan Yu, and Jeremy L O'Brien. Silica-on-silicon waveguide quantum circuits. *Science*, 320(5876):646–649, 2008.

[12] Thomas Gerrits, Nicholas Thomas-Peter, James C Gates, Adriana E Lita, Benjamin J Metcalf, Brice Calkins, Nathan A Tomlin, Anna E Fox, Antía Lamas Linares, Justin B Spring, et al. On-chip, photon-number-resolving, telecommunication-band detectors for scalable photonic information processing. *Physical Review A*, 84(6):060301, 2011.

[13] Robert H Hadfield. Single-photon detectors for optical quantum information applications. *Nature photonics*, 3(12):696–705, 2009.

[14] Bahaa EA Saleh and Malvin Carl Teich. *Fundamentals of photonics*, volume 22. Wiley New York, 1991.

[15] M. A. Pooley, D. J. P. Ellis, R. B. Patel, A. J. Bennett, K. H. A. Chan, I. Farrer, D. A. Ritchie, and A. J. Shields. Controlled-not gate operating with single photons. *Applied Physics Letters*, 100(21), 2012.

[16] C Varnava, RM Stevenson, J Nilsson, J Skiba-Szymanska, B Dzurňák, M Lucamarini, RV Penty, I Farrer, DA Ritchie, and AJ Shields. An entangled-led driven quantum relay over 1 km. *arXiv preprint arXiv:1506.00518*, 2015.

[17] Sacha Kocsis, Guo-Yong Xiang, Tim C Ralph, and Geoff J Pryde. Heralded noiseless amplification of a photon polarization qubit. *Nature Physics*, 9(1):23–28, 2013.

[18] A Zavatta, J Fiurášek, and M Bellini. A high-fidelity noiseless amplifier for quantum light states. *Nature Photonics*, 5(1):52–60, 2011.

[19] AJ Bennett, JP Lee, DJP Ellis, T Meany, E Murray, F Floether, JP Griffths, I Farrer, DA Ritchie, and AJ Shields. Cavity-enhanced coherent light scattering from a quantum dot. *arXiv preprint arXiv:1508.01637*, 2015.